Separation Science and Technology
Publication details, including instructions for authors and subscription information:
http://www.informaworld.com/smpp/title~content=t713708471

Actual Concentration Profiles in Membrane Permeation

Sang Nim Kim[a]; Karl Kammermeyer[a]
[a] UNIVERSITY OP IOWA, IOWA

To cite this Article Kim, Sang Nim and Kammermeyer, Karl(1970) 'Actual Concentration Profiles in Membrane Permeation', Separation Science and Technology, 5: 6, 679 — 697

To link to this Article: DOI: 10.1080/00372367008055530

URL: http://dx.doi.org/10.1080/00372367008055530

SEPARATION SCIENCE, 5(6), pp. 679–697, December, 1970

Actual Concentration Profiles in Membrane Permeation

SANG NIM KIM and KARL KAMMERMEYER
UNIVERSITY OF IOWA
IOWA CITY, IOWA 52240

Summary

The concentration profiles and the concentration dependent diffusion coefficient, at steady-state liquid permeation, were investigated in plastic films by directly measuring the concentration profile. A stacked film packet was developed which permitted peeling of film sections and measuring incremental concentration of permeate. The membrane-permeate systems studied were: nylon 6–water, nylon 6–dioxane, cellulose acetate–water, and polyethylene–dioxane. Membrane thickness was varied from 2 to 53 mil and temperature from 35 to 75°C. Also, poylethylene–benzene and polyethylene–*n*-hexane systems were studied at 17 mil and 35°C only.

The analysis of the experimental data showed that the exponential model, $D = D_0 e^{\alpha C}$, represented the directly measured concentration profiles to a satisfactory degree. The use of this exponential model leads to a linear variation of the diffusion coefficient with distance within the membrane, but nonlinear as a function of concentration.

In mass transfer operations, such as diffusional processes, the driving force is usually a concentration gradient. Normally, one has a knowledge of the over-all driving force. In most diffusional processes there are, however, several resistances in series and it is desirable to know the magnitude of these resistances. This in turn requires a knowledge of the concentration gradients. When these are known, it is possible to formulate a pretty good model which represents the diffusional flow mechanism. A recent study by Hwang (*2*) on the permeation of oxygen through a silicone rubber barrier from oxygen dissolved in water on one side to water on the other side of the barrier demonstrates how one can use experimental data to estimate the respective resistances on the barrier surfaces and the resistance of flow through the barrier. The present investigation is concerned primarily with a study of the concentration gradients in polymeric barriers for single component flow in liquid permeation as originally described by Binning (*1*). No attempt was made to estimate interfacial resistances either on the upstream or downstream side of the barrier.

MODEL STUDIES

Long and co-workers (*3–5*) have calculated concentration gradients for polymeric films from desorption measurements and permeation flux at steady state. They considered the case of the so-called liquid permeation where a liquid is in contact with one face of the barrier and the vapor is removed from the other side of the barrier, usually under vacuum conditions. The information is presented as a plot of a calculated concentration gradient versus the thickness of the membrane. It was necessary, however, to intuitively assume that the barrier side in direct contact with the liquid had reached an equilibrium concentration which could be determined by static equilibrium experiments. So, when the concentration gradient curves are plotted for different thicknesses, one obtains a family of curves which all start at a given point representing the upstream concentration and terminate in another point which corresponds to a down-stream concentration.

EXPERIMENTAL GRADIENTS

While model studies are of great interest and certainly helpful in the interpretation of the flow mechanism, it was felt that experimental determination of actual concentration gradients is a necessity. To accomplish this, a sandwich or film-stack method was developed which permitted the determination of the permeate concentration in individual film layers. It was thus possible to obtain incremental concentration points which could be plotted as a function of film thickness.

Rosenbaum and Cotton (*6*) used a multilayer technique in their reverse osmosis experiments. However, we were not aware of their work while we perfected our scheme; the date of their publication indicates that their and our work was carried on simultaneously. Naturally, the use of this idea is a rather simple concept which should occur to anyone interested in measuring concentration profiles.

To obtain reliable and reproducible results, however, requires careful operation and attention to possible sources of error. We feel that our method has yielded very good data and thus is valuable for further studies in this area. Rosenbaum and Cotton obtained only a single concentration profile in cellulose acetate which showed a straight-line gradient. In all of our experiments, however, we obtained profiles with some degree of curvature.

EXPERIMENTAL PROCEDURE

Preparation of Film Stacks

The preparation of film stacks (sandwich construction) is as follows: Desired layers of thin membranes, such as 1 or 2 mils thick, are stacked one by one, with care to maintain dust-free condition. As each membrane is added to the stack, it is rubbed horizontally with a cloth to squeeze out the air trapped in the interlayers. After all of the desired layers are stacked, they are pressed for 4 to 8 hr with a hydraulic press (Carver Laboratory press) whose plate surfaces are uniformly heated and well insulated. The pressure applied is about 20,000 lb/in.^{2} and the temperature is kept below 60°C. The multilayer membrane thus prepared has the individual layers tightly sandwiched without voids. Yet, it is possible to peel them apart for evaluation at the end of each experiment.

In our present work the multilayer membranes were qualitatively examined with an x-ray diffractometer (General Electric, XR D-5) for any change in the polymer structure due to the pressing. The x-ray diffraction patterns showed no change in the patterns between the laminated membranes and those not laminated. Nylon 6, polyethylene, and cellulose acetate membranes were tested in this manner.

It was felt that the polymer membranes obtained for the tests might possess a skin that had a structure different from the central core, which would introduce an undesired variable. Therefore, the multilayer membranes were tested for possible interlayer resistance effect. For example, a nylon 6 multilayer membrane of 31.9 mils was prepared from 25 layers of 1 mil thick films (nominal thickness) and another one 31.4 mils thick was prepared from 15 layers of 2 mil films. The permeabilities and the concentration distribution at steady-state of the two laminated membranes were established and compared. The identical test was repeated for cellulose acetate membranes and polyethylene membranes. A close check of the experimental results indicated that the interface resistance effect, if any, was negligible.

After a run was completed, the peeled sections were immediately placed into a weighing bottle and the "wet" weight determined. The solvent was then evaporated from the opened weighing bottle at a temperature of 60 to 65°C. Higher temperatures, such as the 80°C used by Rosenbaum and Cotton (*6*), seemed to give some evaporation of film components, such as plasticizers. When constant weight was reached, this weight was used as that of the "dry" film.

Mettler balances weighing to 10^{-6} and 10^{-4} g, respectively, gave satisfactory accuracy in the weight determinations, except for the polyethylene–water system.

When the permeate concentration is greater than 0.005 g permeate/g of dry membrane, the gravimetric method gives satisfactory data.

Permeation Equipment

The film stacks, as shown in Fig. 1, are inserted in a flanged cell, open at the top and closed at the bottom, connected to a vacuum

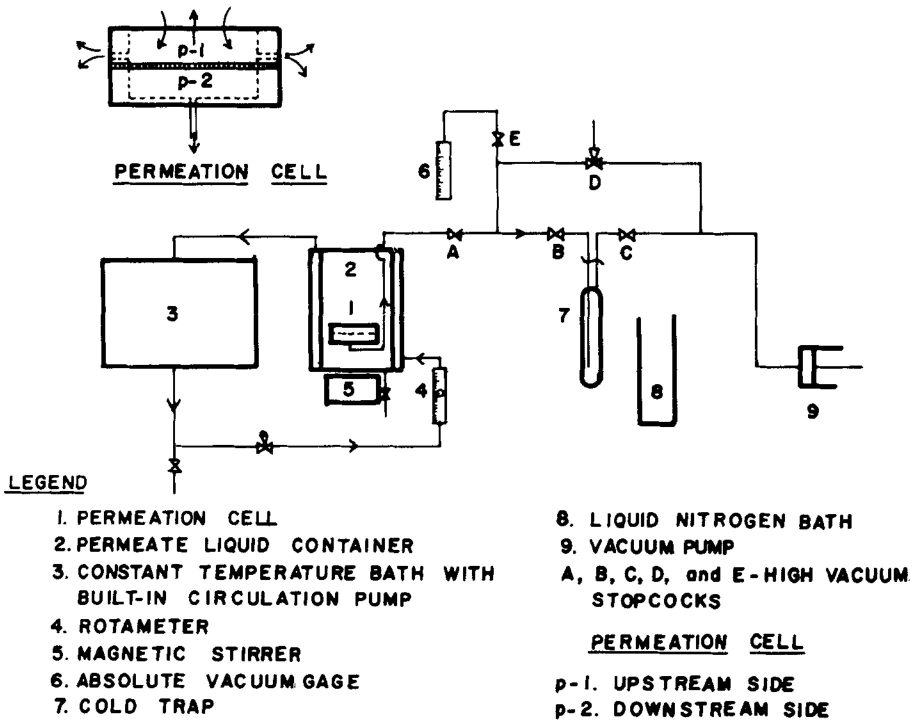

FIG. 1. Schematic diagram of apparatus.

system. The whole cell is submerged in the liquid mixture to be investigated. Steady-state flow is attained by waiting a sufficient length of time after the vacuum is applied on the downstream side. Temperature is controlled by an appropriate bath arrangement.

Systems Covered

The polymer–liquid systems and parameters investigated are as follows:

1. Nylon 6–water.
2. Nylon 6–dioxane.
3. Cellulose acetate–water.
4. Polyethylene–dioxane.

Parameters: All of these systems at 35°C with variation of thickness from 8 to 50 mils (nominal); at 55 and 75°C with one thickness only (17 mils).

Systems 1, 2, and 3 did not exhibit any appreciable degree of swelling of polymer. There was slight swelling in System 4.

5. Polyethylene–hexane.
6. Polyethylene–benzene.

Parameters: Systems 5 and 6 only at 35°C and one thickness (17 mils).

Systems 5 and 6 exhibited appreciable swelling of polymer.

Properties of polymer films and permeating liquids are listed in Tables 1 and 2.

TABLE 1

Characteristics of Membranes

Membrane	Supplier	Sp gr	Crystallinity (%)
Nylon 6	Allied Chem. Corp. Code, Capran Type 77-C	1.123	59
Cellulose acetate[a]	Celanese Plastics Co. Code, P-912	1.30	Very low
Polyethylene	DuPont Code, A-101	0.926	55

[a] Acetate value: 39.2 ± 0.3% of unplasticized flake weight. Plasticizer: diethyl phthalate, 20.8% of total weight.

An attempt was made with the system polyethylene–water but the concentration gradient was so low that the gravimetric procedure failed.

TABLE 2

Properties of Liquids

Liquid	Grade	Mol wt	Sp gr (at 4°C)	Molecular structure	Mp (°C)	Bp (°C)
Water	Dist	18.00	1.000	H_2O	0.0	100.0
p-Dioxane	Reag	88.10	1.035	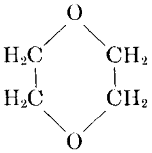	11.7	101.5
Benzene	Reag	78.11	0.879		5.5	80.1
n-Hexane	Reag	86.17	0.660	$CH_3(CH_2)_4CH_3$	−94.3	69.0

Operating Procedure (see Fig. 1)

A laminated membrane was mounted in the permeation cell and the assembly was tested for leaks. Approximately 2 liters of permeate were heated in the permeate container and maintained at test temperature with an accuracy of ±0.2°C. When the temperature was stabilized, the permeation cell was immersed into the permeate bath. Vacuum was applied to the downstream side with the stopcocks A, B, and C in Fig. 1 open. The operating pressure on the downstream side was kept at 50 μ abs or less in all experiments.

The time required to reach steady-state permeation (i.e., when the concentration distribution of the permeate in the membrane no longer changes with time) was obtained by running a series of preliminary experiments with varying test times and evaluation of the concentration distribution in the membrane. This time varied from 7 to 70 hr depending on the permeate, its temperature, and the thickness of the membrane.

When steady-state permeation was reached, the trap was immersed in liquid nitrogen and remained there throughout the experiment. The permeate was captured in the cold trap. At the end of the experiment, the stopcocks B and C were closed and D was opened to the vacuum pump to maintain the vacuum in the downstream side. The elapsed time was measured from the moment the trap was immersed in liquid nitrogen to the closing of the stopcocks (B and C) and this was used as the test time.

At the end of the experiment, the trap and the permeate collected in it were allowed to reach room temperature, disconnected quickly, and weighed. Then, 3 to 4 square inches of the membrane were cut out, the membrane was quickly peeled apart, the sections were placed individually into weighing bottles, and the wet weight of the membrane was taken. The permeate in each membrane was then evaporated from the open weighing bottle, at 60°C for the cellulose acetate membrane and at 65°C for the nylon 6 and polyethylene membranes. When constant weight was reached, it was used as that of the dry membrane. Thus, each data point in each curve represents the average concentration of each layer.

The thickness of the membrane was measured to 0.1 mil (0.0001 in.) at five representative positions across the effective permeation area of the membrane. An average was used in the calculations.

The static equilibrium concentrations of the permeates in the membranes were measured by a method similar to the ASTM method of testing water absorption of plastics (ASTM Designation: D 570-63). Six to 7 square inches of the membranes were cut and immersed totally in a permeate at the test temperature for 48 hr or longer. The samples were then removed from the permeate one at a time, the free permeate liquid on the membrane surface was blotted with a dry paper towel, the sample was immediately placed into a tared weighing bottle, and the wet weight was taken. The permeate in the membrane was then evaporated from the open weighing bottle at 60°C for cellulose acetate membrane and at 65°C for the nylon 6 and polyethylene membranes. When constant weight was reached, it was used for that of the dry weight. The blotting was done quickly and consistently for all the samples. Usually 10 samples were tested and averaged for each value.

EXPERIMENTAL RESULTS

The data obtained consist of concentration gradients of the permeating fluid and total flux determination, both under steady-state conditions, and static equilibrium concentration C^* of permeate in the polymer film. Thickness of film stacks and temperature of operation were varied.

The findings can be summarized as follows:

Concentration Profiles

System 1: Nylon 6–water. Figure 2 presents C vs. x_f for different thicknesses L. Figure 3 presents C vs. x_f at one thickness for different temperatures.

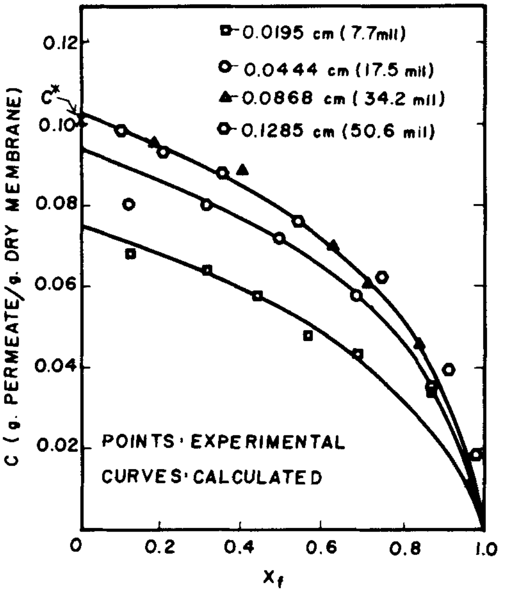

FIG. 2. Concentration profile of nylon 6-water at 35°C for variation of total membrane thickness.

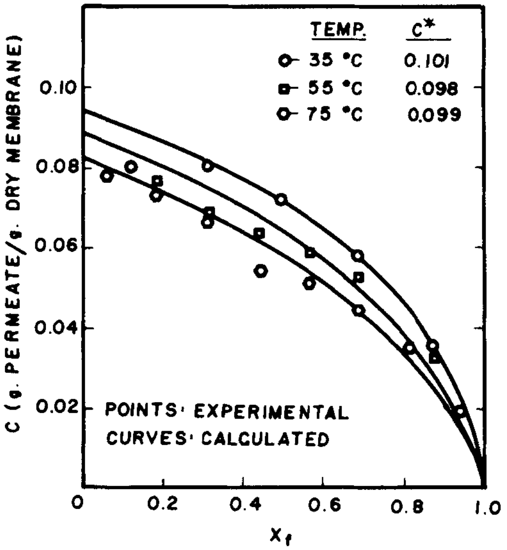

FIG. 3. Concentration profile of nylon 6-water for variation of temperature. Membrane thickness: 0.0432 cm (17 mil).

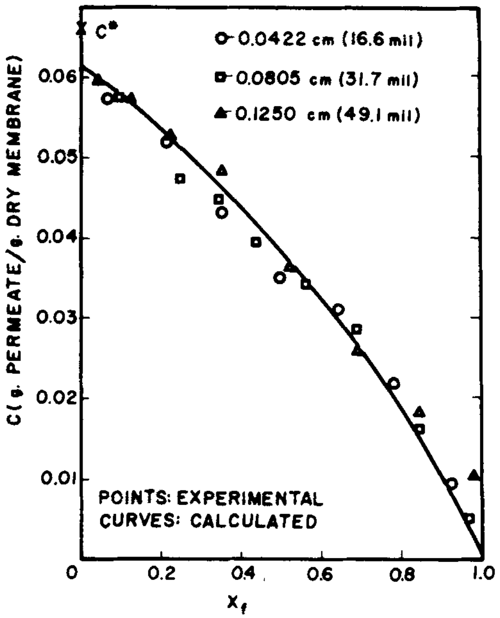

FIG. 4. Concentration profile of cellulose acetate–water at 35°C for variation of total membrane thickness.

System 2: Nylon 6–dioxane. C vs. x_f, same behavior as System 1 for both variation in L and temperature.

System 3: Cellulose acetate–water. Figure 4 presents C vs. x_f for varying thicknesses and shows that all thicknesses fall on the same curve. The temperature behavior is analogous to System 1 (Fig. 3).

System 4: Polyethylene–dioxane. C vs. x_f same behavior as System 1 (Fig. 2). Figure 5 presents C vs. x_f at one thickness with variation of temperature; note that the order is reversed compared to other systems as represented by Fig. 3.

Systems 5 and 6: Polyethylene with hexane and benzene was investigated only at 35°C and a 17-mils thick stack. The results are shown in Fig. 6 with the corresponding dioxane data. The permeation flux data are given and show that there is no direct relationship between flux and magnitude of the concentration profile as far as a comparison of the different systems is concerned.

Qualitatively, the distances between C^* and C_1 values give an indication of the respective resistance relationships. Thus C^* and C_1

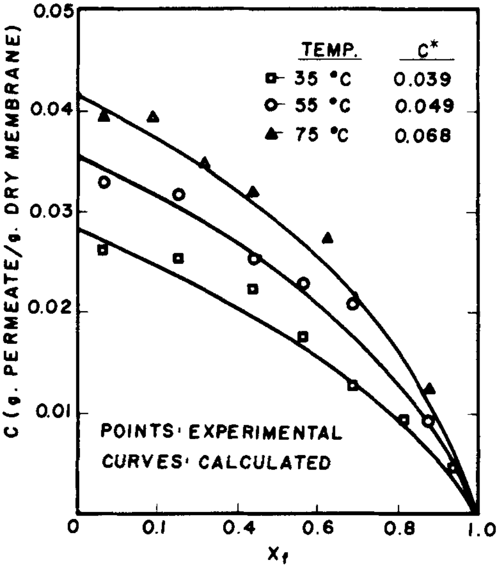

FIG. 5. Concentration profile of polyethylene–dioxane for variation of temperature. Membrane thickness: 0.0432 cm (17 mil).

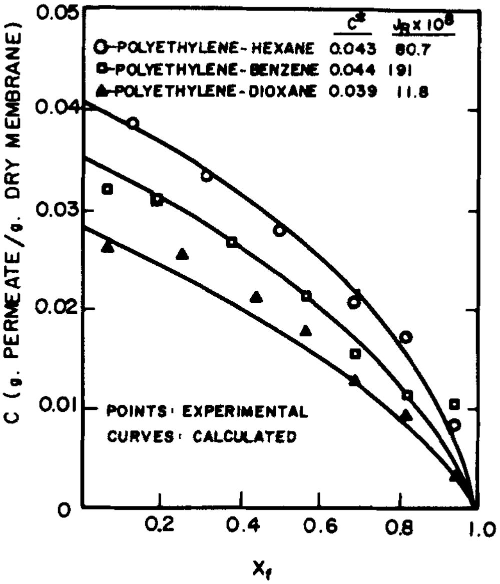

FIG. 6. Concentration profile at 35°C for polyethylene–various permeates. Membrane thickness: 0.0432 cm (17 mil).

for hexane are quite close, indicating that diffusion resistance in the polymer controls the over-all permeation process. The gap between the C^* and C_1 values for benzene and dioxane is sufficiently large so that one must conclude that the resistance at the liquid–polymer interface exerts an appreciable influence.

Equilibrium Concentration

The values of equilibrium concentration C^* are summarized in Table 3. Evidently, the temperature effect is not uniform. Water in nylon 6 is essentially unaffected. Dioxane in nylon 6 does not vary a great deal; the absolute values are rather low and thus less accurate. Water in cellulose acetate shows a decrease with increasing temperature, while dioxane in polyethylene shows an increase. No apparent explanation is available for this difference in behavior. It is interesting that Long (*5*) reports the C^* values for *n*-heptane, methyl-

TABLE 3

C^*, α, and D_0 Values

System	Membrane	Permeate	Temp (°C)	(g permeate/g dry membrane) C^* [a]	Per cent standard deviation of C^*	α [b]	$D_0 \times 10^8$ [b]
1	Nylon 6	Water	35	0.101	4.4	27.7	0.20
	"	"	55	0.098	3.5	24.3	1.62
	"	"	75	0.099	3.3	23.6	8.13
2	Nylon 6	Dioxane	35	0.0113	13.6	86.3	14.5
	"	"	55	0.0161	10.6	82.7	39.5
	"	"	75	0.0196	13.2	100	59.1
3	Cellulose acetate	Water	35	0.066	6.8	17.4	9.2
	"	"	55	0.055	8.5	32.6	23.1
	"	"	75	0.051	6.5	47.0	65.6
4	Polyethylene	Dioxane	35	0.039	5.1	39.5	9.0
	"	"	55	0.049	8.6	54.1	29.4
	"	"	75	0.068	10.0	55.7	72.0
5	Polyethylene	Hexane	35	0.043	7.2	47.4	26.8
6	Polyethylene	Benzene	35	0.044	6.1	41.9	102

[a] For each C^* value, 9 to 11 samples were tested and averaged.

[b] Obtained by least-square fitting.

cyclohexane, and toluene in polypropylene also increase with rising temperature.

Permeation Flux and Permeability

The experimental results are summarized in Table 4. The amounts of permeated liquid, removed as vapor at about 50 μ downstream pressure, were collected in the frozen state in the liquid nitrogen trap. The permeation flux J_l represents the amounts collected per unit barrier area and unit time. The permeability $P_l = (J_l)\ (\Delta L/\Delta C_b)$ is a phenomenological coefficient on the basis of the over-all driving force. It is therefore dependent upon thickness when the resistance at the polymer–liquid interface is not negligible. This is shown in Table 4 for Systems 1, 2, and 4 at the 35°C level. As indicated previously, in System 3 the diffusion resistance within the polymer completely controls the flow of permeate. Thus the P_l values should be essentially constant and this is shown for System 3 in Table 4.

Significance of Data

Variation of Thickness. *Membrane Thickness:* The thicknesses of the membrane stacks were determined by the availability of thin films of the respective polymers and the desire to obtain a sufficient number of experimental data points for concentration distribution. The aim was to obtain 7 to 8 points. So, where films of 1 mil thickness were available, the stacks contained as few as 8 layers and up to 24 layers. Most of the thicker stacks were made from 2 mils thick films. Cellulose acetate film was available in 2 mils thickness only, and therefore the thinnest stack which could be built was almost 17 mils thick.

Experimental Results: Systems 1, 2, and 4 show that a critical thickness value was observed within the range of thickness investigated—see Fig. 2 as being representative of the behavior.

In System 3, Fig. 4, even the thinnest stack which was examined was above some critical thickness. Actually, the permeation flux was obtained for films of 2 and 4 mils thickness. It was found that even at these thicknesses the flux was still inversely proportional to thickness. Thus, the points for 2 and 4 mil, if they could have been determined, would still have fallen on the same curve. It is safe to conclude that a change in relative resistances would be found at very low thicknesses (perhaps 1 mil or less).

TABLE 4

Over-all Flux J_l, Permeability P_l, and Effective Diffusion Coefficient $\bar{D}_t$ (Pressure drop: 1 atm)

System	Membrane	Permeate	Temp (°C)	Thickness, cm (mil)	$J_l \times 10^8$ (g/sq cm-sec)	$P_l \times 10^9$ (g-cm/sq cm-sec)	$\bar{D}_t \times 10^8$ (sq cm/sec)
1	Nylon 6	Water	35	0.0051(2.0)	7.88	0.41	—
	"	"	35	0.0104(4.1)	4.08	0.43	—
	"	"	35	0.0195(7.7)	2.61	0.51	0.66
	"	"	35	0.0444(17.5)	1.84	0.82	0.94
	"	"	35	0.0868(34.2)	1.32	1.15	1.09
	"	"	35	0.1285(50.6)	0.96	1.25	1.10
	"	"	55	0.0437(17.2)	11.5	5.11	5.70
	"	"	75	0.0439(17.3)	45.8	21.1	24.7
2	Nylon 6	Dioxane	35	0.0051(2.0)	23.0	1.11	—
	"	"	35	0.0104(4.1)	13.0	1.30	—
	"	"	35	0.0264(10.4)	6.0	1.55	20.7
	"	"	35	0.0427(16.8)	4.88	2.01	22.5
	"	"	35	0.0800(31.5)	3.68	2.84	25.2
	"	"	35	0.1282(50.5)	2.81	3.17	24.8
	"	"	55	0.0427(16.8)	8.77	3.61	53.5
3	Cellulose acetate	Water	35	0.0051(2.0)	205	10.51	—
	"	"	35	0.0104(4.1)	97.6	10.31	—
	"	"	35	0.0422(16.6)	24.6	10.43	16.5
	"	"	35	0.0805(31.7)	11.9	9.67	16.5
	"	"	35	0.1247(49.1)	7.56	9.57	16.5
3	Cellulose acetate	Water	55	0.0422(16.6)	64.3	27.5	56.2
	"	"	75	0.0419(16.5)	161	69.2	180
4	Polyethylene	*p*-Dioxane	35	0.0051(2.0)	45.1	2.17	—
	"	"	35	0.0104(4.1)	24.1	2.40	—
	"	"	35	0.0297(11.7)	14.7	4.20	15.4
	"	"	35	0.0414(16.3)	11.8	4.75	16.7
	"	"	35	0.0795(31.3)	8.92	6.84	20.9
	"	"	35	0.1323(53.1)	5.42	6.91	20.9
	"	"	55	0.0419(16.5)	75.7	30.6	89.1
	"	"	75	0.0422(16.6)	175	112	281
5	Polyethylene	*n*-Hexane	35	0.0414(16.3)	80.7	50.6	81.9
6	Polyethylene	Benzene	35	0.0427(16.8)	191	92.8	231

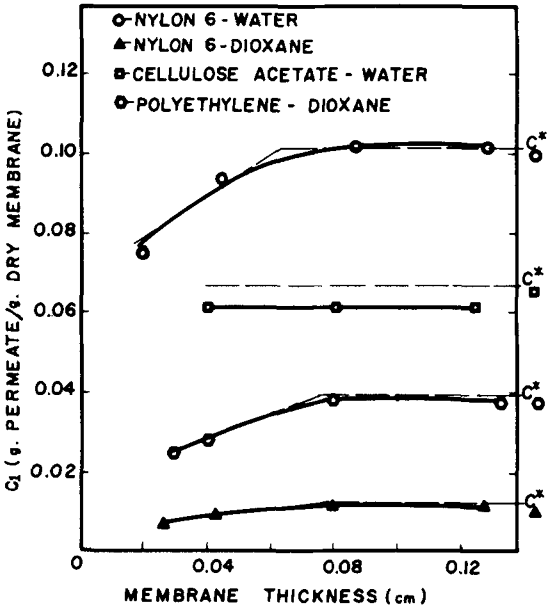

FIG. 7. Permeate concentration at interface 1 (C_1) for variation of total membrane thickness at 35°C.

The explanation of the behavior exhibited in Fig. 2 is rather obvious. It is illustrated graphically in Fig. 7, where the surface concentration at the liquid–film interface, C_1, is plotted against membrane thickness L. Above a critical thickness, L_{crit}, the diffusional resistance within the membrane evidently becomes sufficiently large so that it controls the flow mechanism. Below L_{crit} the resistance at the liquid–polymer interface begins to exert a greater and greater influence as the thickness decreases. The significant parameter is the relative magnitude of the respective resistances and not their absolute values. Thus, a significant point is that the surface concentration of the permeate C_1 becomes less than the static equilibrium concentration C^*, as shown in Fig. 8.

What this means is that the permeate diffuses within the film at a rate faster than it is available at the film surface. This behavior is entirely logical and it was shown in Hwang's study (*2*) that the diffusional resistance of a silicone barrier to the flow of oxygen was only about 11% of the total flow resistance in his system, and the major portion of the over-all resistance was encountered at the interfaces.

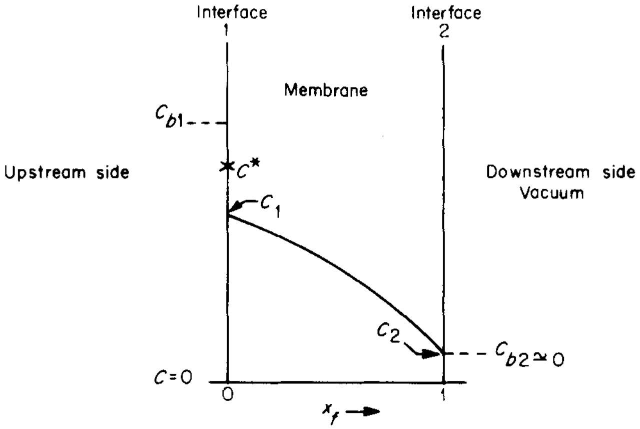

FIG. 8. Concentration profile.

In the present liquid permeation study, the situation is analogous. Thus, resistances are present at the liquid–polymer and the polymer–vapor interfaces. The data do not permit any conclusion as to the relative magnitudes of these resistances.

Variation of Temperature. Many systems could be expected to show the behavior illustrated in Fig. 3. That is, as the operating temperature increases the concentration profile becomes less steep because the diffusional resistance within the polymer film decreases with increasing temperature. This also means that the diffusion rate increases.

In contrast, the polyethylene–dioxane system gave the opposite trend. The concentration gradient in the film was greatest at the highest temperature examined (75°C). A preliminary interpretation ascribes this behavior to the relative changes in interface resistance and diffusion resistance as the temperature increases. The four systems that were investigated for both temperature and thickness variation showed several modes of behavior. It is evident that many more systems of solvent–polymer combinations will have to be examined before more rigorous interpretations can be formulated.

THEORETICAL INTERPRETATION

By using the basic differential equation for diffusion and the equation for the permeation flux in the x-direction only, it is possible to formulate the following expressions for steady-state conditions:

$$J = -\frac{D}{L}\frac{dC}{dx_f} \qquad \text{for} \qquad 0 \leq x_f \leq 1 \tag{1}$$

$$\frac{d}{dx_f}\left(D\frac{dC}{dx_f}\right) = 0 \qquad \text{for} \qquad 0 \leq x_f \leq 1 \tag{2}$$

where the boundary conditions are $C = C_1$ at $x_f = 0$, and $C = C_2 \simeq 0$ at $x_f = 1$.

If, in addition, one accepts an exponential model of the diffusivity, suggested by a number of other investigators:

$$D = D_0 \exp(\alpha C) \tag{3}$$

it is possible to derive the following equations by combining Eqs. (1), (2), and (3):

For *concentration profile:*

$$C = \frac{1}{\alpha} \ln\left[(1 - e^{\alpha C_1})x_f + e^{\alpha C_1}\right] \tag{4}$$

Note that the profile should be independent of D_0.

$$\frac{dC}{dx_f} = \left(\frac{1}{\alpha}\right)\frac{1 - e^{\alpha C_1}}{(1 - e^{\alpha C_1})x_f + e^{\alpha C_1}} \tag{5}$$

For *diffusion coefficient:*

$$D = D_0[(1 - e^{\alpha c_1})x_f + e^{\alpha C_1}] \qquad \text{for} \qquad 0 \leq x_f \leq 1 \tag{6}$$

$$\frac{dD}{dx_f} = D_0(1 - e^{\alpha C_1}) \tag{7}$$

According to Eq. (7) the diffusion coefficient varies linearly inside the membrane. Its slope is $[D_0(1 - e^{\alpha C_1})]$ and its values are $[D_0 e^{\alpha C_1}]$ at $x_f = 0$, and D_0 at $x_f = 1$. Values of α and D_0 determined by a least-square fitting are listed in Table 3.

The use of the exponential model leads to a linear variation of the diffusion coefficient as a function of distance within the membrane. Figure 9 shows such a plot for the system nylon 6–water. Also shown in Fig. 9 is that the diffusion coefficient varies as a logarithmic function of the concentration inside the membrane. The curves for the other systems would be entirely analogous.

Utility of Equations

The equations could be used in a predictive manner, if one were able to determine values of α, D_0, and C_1, by methods that would not require a stack experiment. For instance, as shown by Long (*5*), some

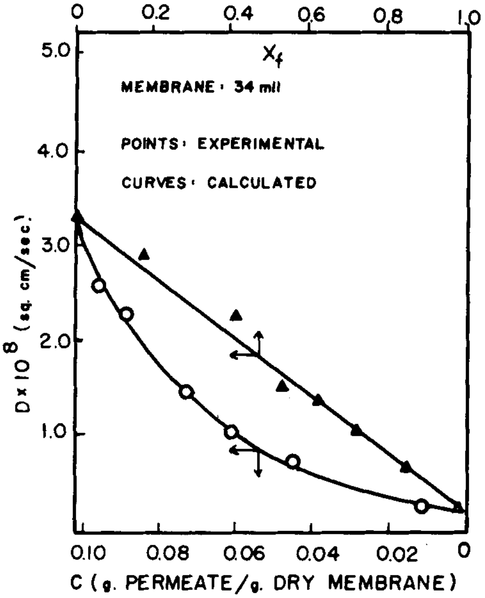

FIG. 9. Diffusion coefficients at 35°C for nylon 6–water.

values of α and D_0 can be determined from a desorption experiment and a permeation flux determination at steady-state; both of these experiments would be simpler than a stack experiment.

However, at present we do not know if the α and D_0 values obtained in such a manner would give values for these parameters that would agree with values obtained by our procedure. Furthermore, Long's procedure does not cover the situation where the surface concentration C_1 is not equal to the static equilibrium concentration C^*. Somewhat fortuitously our results have already shown that $C_1 = C^*$ only when a film becomes sufficiently thick so that it exceeds the critical thickness value L_{crit}.

Therefore, the present utility of the equations is rather limited because they serve only to express the experimental curves mathematically. The potential utility is obviously sufficiently attractive so that our own studies are continuing with particular emphasis on parameter determination.

CONCLUSIONS

The simple exponential model $D = D_0 e^{\alpha C}$ represents the experimental concentration profiles to a satisfactory degree. These profiles show that there is, in general, a greater resistance to diffusion on the downstream side than at the upstream side. No case was observed in which the concentration gradient at the downstream side was so steep that essentially all the resistance to diffusion existed there, as predicted by Binning (*1*) and reported by Long (*5*). Also, the experimental results reveal that only for the systems in which the resistance in the polymer membrane controls the over-all permeation rate are the concentration profiles independent of the membrane thickness and the permeability inversely proportional to the membrane thickness.

For all the systems investigated, the diffusion coefficient increased as the permeate concentration inside the membrane increased. From the downstream side to the upstream side of a membrane, the diffusion coefficient showed a 5- to 15-fold change. The gravimetric method of obtaining the permeate concentration yielded satisfactory results when the concentration was larger than about 0.005 g permeate/g dry membrane. However, the multilayer membrane technique as such is not limited in its application. By utilizing radioactive isotopes and an effective means of counting them, this method can be applied to systems of low permeate concentrations, and also of binary mixtures.

Acknowledgment

The partial support of this study by the National Science Foundation is gratefully acknowledged.

Nomenclature

α	constant (g dry membrane/g permeate)
C	permeate concentration in membrane (g permeate/g dry membrane)
C_b	bulk concentration (g permeate/cc)
C^*	static equilibrium permeate concentration in membrane (g permeate/g dry membrane)
C_1	permeate concentration in membrane at the Interface 1 at steady state (g permeate/g dry membrane)
C_2	permeate concentration in membrane at the Interface 2 at steady state (g permeate/g dry membrane)
D	diffusion coefficient (sq cm/sec)
D_0	diffusion coefficient at zero concentration (sq cm/sec)
$\bar{D}_t$	effective diffusion coefficient $\left[\bar{D}_t = \frac{D_0}{C_1}\int_0^{C_1} e^{\alpha C}\,dC\right]$ (sq cm/sec)

Interface 1	the interface between the permeate charge and the upstream side surface of membrane
Interface 2	the interface between the down-stream side surface of the membrane and the down-stream side
L	total thickness of membrane (cm)
J_l	permeation flux (g/sq cm-sec)
P_l	permeability $\dfrac{\text{g-cm}}{\text{sec-sq cm} - (\text{g permeate/cc})}$
x	distance in membrane from Interface 1 (cm)
x_f	fraction of membrane thickness (x/L)

REFERENCES

1. R. C. Binning, R. J. Lee, J. F. Jennings, and E. C. Martin, *Ind. Eng. Chem.,* **53**(1), 45–50 (1961).

2. S. T. Hwang, T. E. S. Tang, and K. Kammermeyer, *Amer. Chem. Soc. Polym. Preprints,* **10**(2), 978 (New York Meeting, September, 1969).

3. N. N. Li and R. B. Long, *A.I.Ch.E. J.,* **15**(1), 73–80 (1969).

4. N. N. Li, R. B. Long, and E. J. Henley, *Ind. Eng. Chem.,* **57**, 18–29 (1965).

5. R. B. Long, *Ind. Eng. Chem., Fundam.,* 4(4), 445–451 (1965).

6. S. Rosenbaum and O. Cotton, *J. Polymer. Sci., Part A-1,* **7**, 101–109 (1969).

Received by editor March 13, 1970